

# Moving Matter: Efficient Reconfiguration of Tile Arrangements by a Single Active Robot

**Aaron T. Becker** ✉ 

Electrical Engineering, University of Houston, Texas, USA

**Sándor P. Fekete** ✉ 

Computer Science, TU Braunschweig, Germany

**Jonas Friemel** ✉ 

Electrical Engineering and Computer Science, Bochum University of Applied Sciences, Germany

**Ramin Kosfeld** ✉ 

Computer Science, TU Braunschweig, Germany

**Peter Kramer** ✉ 

Computer Science, TU Braunschweig, Germany

**Harm Kube** ✉ 

Computer Science, TU Berlin, Germany

**Christian Rieck** ✉ 

Discrete Mathematics, University of Kassel, Germany

**Christian Scheffer** ✉ 

Electrical Engineering and Computer Science, Bochum University of Applied Sciences, Germany

**Arne Schmidt** ✉ 

Computer Science, TU Braunschweig, Germany

---

## Abstract

We consider the problem of reconfiguring a two-dimensional connected grid arrangement of passive building blocks from a start configuration to a goal configuration, using a single active robot that can move on the tiles, remove individual tiles from a given location and physically move them to a new position by walking on the remaining configuration. The objective is to determine a reconfiguration schedule that minimizes the overall makespan, while ensuring that the tile configuration remains connected. We provide both negative and positive results. (1) We present a generalized version of the problem, parameterized by weighted costs for moving with or without tiles, and show that this is NP-complete. (2) We give a polynomial-time constant-factor approximation algorithm for the case of disjoint start and target bounding boxes. In addition, our approach yields optimal carry distance for 2-scaled instances.

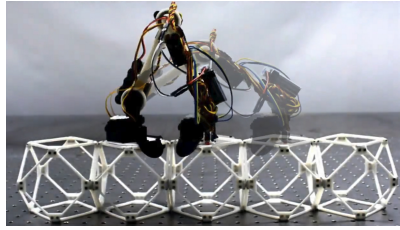
**2012 ACM Subject Classification** Theory of computation → Computational geometry

**Keywords and phrases** Programmable matter, Reconfiguration, Polyominoes, Assembly, Path planning, Approximation, NP-completeness

**Funding** Work from TU Braunschweig and HS Bochum was partially supported by the German Research Foundation (DFG), project “Space Ants”, FE 407/22-1 and SCHE 1931/4-1. Work from the University of Kassel was partially supported by DFG grant 522790373.

## 1 Introduction

Building and modifying structures consisting of many basic components is an important objective, both in fundamental theory and in a spectrum of practical settings. Transforming such structures with the help of autonomous robots is particularly relevant in very large [14] and very small dimensions [38] that are hard to access for direct human manipulation, e.g., in



■ **Figure 1** A simple BILL-E robot that can move on a configuration of digital, light-weight material and relocate individual voxels for overall reconfiguration. Photo adapted from [29].

extraterrestrial space [9, 31] or in microscopic environments [7]. This gives rise to the natural algorithmic problem of rearranging a given start configuration of (potentially very many) *passive* objects by a relatively small set of *active* agents to a desired target configuration. Performing such reconfiguration at scale faces a number of critical issues, including (i) the cost and weight of materials, (ii) the potentially disastrous accumulation of errors, (iii) the development of simple yet resilient agents to carry out the active role, and (iv) achieving overall feasibility and efficiency.

In recent years, significant advances have been made to deal with these challenges. On the macroscopic side, ultra-light and scalable composite lattice materials [11, 24, 25], address the first issue, making it possible to construct modular, reconfigurable structures with platforms such as NASA’s BILL-E and ARMADAS [30, 28, 24]; the underlying self-adjusting lattice also resolves the issues (ii) of accuracy and error correction, allowing it to focus on discrete, combinatorial structures, consisting of regular tiles (in two dimensions) or voxels (in three dimensions). A further step has been the development of (iii) simple autonomous robots [10, 29] that can be used to carry out complex tasks, as shown in Figure 1: The robot can move on the tile arrangement, remove individual tiles and physically relocate them to a new position by walking on the remaining configuration, which needs to remain connected at all times. This is mirrored on the microscopic scales, where the development of microbots [37] and even nanobots [36] promises fundamentally new approaches to configuring objects and mechanisms, such as forming specific configurations or gathering in designated locations for tasks such as targeted drug delivery [8, 32], again based on discrete, lattice-based structures.

In this paper, we deal with the algorithmic challenge (iv): How can we use such a robot to transform a given start configuration into a desired goal arrangement, as quickly as possible?

## 1.1 Our contributions

We investigate the problem of finding minimum cost reconfiguration schedules for a single active robot operating on a (potentially large) number of tiles. In particular, we obtain the following results for the SINGLE ROBOT RECONFIGURATION problem.

- (1) We present a generalized version of the problem, parameterized by weighted costs for moving with or without tiles, and show that this is NP-complete.
- (2) On the other hand, we give a polynomial-time constant-factor approximation algorithm for the case of disjoint start and target bounding boxes. Our approach yields optimal carry distance for 2-scaled instances.

For precise model and problem descriptions, we refer to Section 1.3.

## 1.2 Related work

Garcia et al. [20, 21] showed that computing optimal schedules for reconfiguring polyominoes with BILL-E bots, see [28] and Figure 1, is in general NP-complete. For tackling the problem, they designed heuristic approaches exploiting rapidly exploring random trees (RRT), and a time-dependent variant of the A\* search algorithm. Furthermore, they used target swapping heuristics to reduce the overall traveled distance in case of multiple BILL-E bots.

A different context for reconfiguration arises from programmable matter [22, 23, 26]. Here, even finite automata are capable of building bounding boxes of tiles around polyominoes, as well as scale and rotate them while maintaining connectivity at all times [17, 35].

When considering active matter, i.e., the arrangement is composed of self-moving objects (or agents), multiple different models exist [5, 6, 12, 34]. For example, in the *sliding cube model* (or the *sliding square model* in two dimensions), first introduced by Fitch et al. [18, 19] in 2003, agents are allowed to make two different moves, namely, sliding along other agents, or performing a convex transition, i.e., moving around a convex corner. Akitaya et al. [3] show that universal sequential reconfiguration in two dimensions is possible, even while maintaining connectivity of all intermediate configurations, but minimizing the makespan of a schedule is NP-complete. Recently, Abel et al. [1] and Kostitsyna et al. [33] independently give similar results for the three dimensional setting. Most recently, Akitaya et al. [4] show that it is NP-complete to decide whether there exists a schedule of makespan 1 in the parallel sliding square model and they provide a worst-case optimal algorithm.

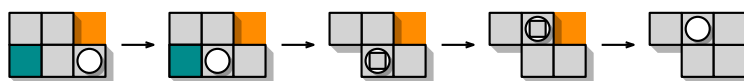
In a slightly more relaxed model, Fekete et al. [15, 16] show that parallel connected reconfiguration of a swarm of (labeled) agents is NP-complete, even for deciding whether there is a schedule of makespan 2. Complementary, they present algorithms for computing constant stretch schedules, i.e., the ratio between the makespan of a schedule and a natural lower bound (the maximum minimum distance between an individual start and target position) is bounded by a constant.

## 1.3 Preliminaries

For the following, we refer to Figure 2. We are given a fixed set of  $n$  indistinguishable square *tile* modules located at discrete, unique positions  $(x, y)$  in the infinite integer grid  $\mathbb{Z}^2$ . If their positions induce a connected subgraph of the grid, we say that the tiles form a *connected configuration* or *polyomino*. Let  $\mathcal{C}(n)$  refer to the set of all polyominoes of  $n$  tiles.



(a) Left to right: The cardinal directions, a robot without and with payload, a tile, and tiles that only exist in either the start or the target configuration, respectively.



(b) A valid schedule to reconfigure the instance to the left. The robot can move on tiles, in cardinal directions. Also, it can pick up and drop off adjacent tiles.

■ **Figure 2** A brief overview of legal operations in our model.

Consider a robot that occupies a single tile at any given time. At each discrete time step, the robot can either move to an adjacent tile, pick up a tile from an adjacent position (if it is not already carrying one), or place a tile at an adjacent unoccupied position (if it is carrying a tile). Tiles may only be picked up if the resulting configuration is valid, i.e., the operation preserves connectivity.

We use cardinal directions to navigate; the unit vectors  $(1, 0)$  and  $(0, 1)$  correspond to *east* and *north*, respectively. Naturally, their opposing vectors extend *west* and *south*.

A *schedule*  $S$  is a finite, connectivity-preserving sequence of operations to be performed by the robot. As the robot's motion is restricted to movements on the polyomino, we refer to distances it travels as *geodesic* distances. Let  $d_C(S)$  denote the *carry distance*, which is the sum of geodesic distances between consecutive pickups and drop-offs in  $S$ . This represents the total distance the robot travels while carrying a tile, with an additional unit of distance added each time the robot either picks up or places a tile. Similarly, the *empty distance*  $d_E(S)$  is the sum of geodesic distances between drop-offs and pickups in  $S$ . We say that  $S$  is a schedule for  $C_s \Rightarrow C_t$  exactly if it transforms  $C_s$  into  $C_t$ .

**Problem statement.** We consider SINGLE ROBOT RECONFIGURATION: Given two connected configurations  $C_s, C_t \in \mathcal{C}(n)$  and a rational weight factor  $\lambda \in [0, 1]$ , determine a schedule  $S$  for  $C_s \Rightarrow C_t$  that minimizes the *weighted makespan*  $|S| := \lambda \cdot d_E(S) + d_C(S)$ . We refer to the minimum weighted makespan for any given instance as OPT.

## 2 Computational complexity of the problem

In this section, we investigate the computational complexity of the decision variant of the generalized reconfiguration problem. In particular, we prove that the problem is NP-complete for any rational factor  $\lambda \in [0, 1]$ . This generalizes a result by Garcia et al. [21], who demonstrate that the problem is NP-complete for the special case of  $\lambda = 1$ .

► **Theorem 1.** *SINGLE ROBOT RECONFIGURATION is NP-complete for any rational  $\lambda$ .*

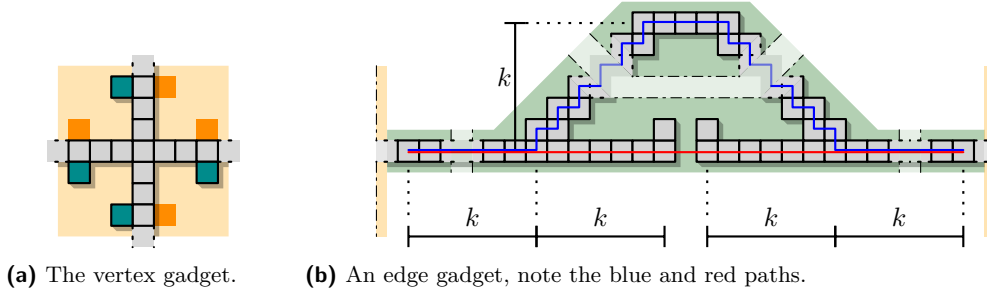
By considering the discrete steps of a schedule individually, we can confirm the moves' validity and certify a schedule's total cost. It follows that the SINGLE ROBOT RECONFIGURATION problem is in NP for any rational  $\lambda \in [0, 1]$ . We distinguish between two cases of (1)  $\lambda \in (0, 1]$  and (2)  $\lambda = 0$  and give separate reductions from two NP-complete problems.

For (1), we reduce from the HAMILTONIAN PATH problem in grid graphs [27], which asks whether there exists a path in a given grid graph that visits each vertex exactly once. We modify a construction previously used by Garcia et al. [21], where the high-level idea is an expansion of the grid graph, placing small reconfiguration tasks at every vertex of the original graph. An "ideal" schedule visits each vertex exactly once.

► **Lemma 2.** *SINGLE ROBOT RECONFIGURATION is NP-complete for  $\lambda \in (0, 1]$ .*

**Proof.** We reduce from the HAMILTONIAN PATH problem in grid graphs [27], which asks us to decide whether there exists a path in a given graph that visits each vertex exactly once. We use a modified variant of the construction described by Garcia et al. [21], defining our start and target configurations based on the gadgets from Figure 3 as follows.

Let  $k \gg 1/\lambda$ . For each vertex of a given grid graph  $G_{in}$ , we create a copy of a  $7 \times 7$  *vertex gadget* that represents a constant-size, locally solvable task, see Figure 3(a). We connect all adjacent vertex gadgets with copies of a  $(k + 1) \times (4k + 3)$  *edge gadget*, as depicted in Figure 3(b). While we reuse the exact vertex gadget from [21], our edge gadget is a little



■ **Figure 3** Our construction forces the robot to visit each vertex gadget at least once, traversing edge gadgets along either the red or the blue path.

more complex. A robot traveling through the gadget has two options, indicated by red and blue paths in Figure 3(b).

The blue path offers a simple, walkable option of  $6k + 2$  empty travel units, while the red path is only available if the robot performs 2 carry steps to construct and deconstruct a unit length bridge at the center, temporarily creating a walkable path of  $4k + 2$  units. This is cheaper exactly if  $\lambda(6k + 2) > \lambda(4k + 2) + 2$ , i.e., if  $k > 1/\lambda$ . Since  $\lambda$  is a rational number, we can pick a value  $k$  that is polynomial in  $\lambda$  and permits a construction in which taking the red path is always cheaper. The blue path thus serves solely for the purpose of providing connectivity and will never be taken by the robot.

An optimal schedule will therefore select a minimal number of edge gadgets to cross, always taking the red path. As vertex gadgets always require the same number of moves to solve, we simply capture the total cost for a single vertex gadget as  $t_g$ . For a graph  $G_{in}$  with  $m$  vertices, an optimal schedule has makespan  $m \cdot t_g + (m - 1) \cdot (4k\lambda + 2\lambda + 2)$  exactly if the underlying graph is Hamiltonian, and greater otherwise.

Given a connected grid graph, such a schedule never builds bridges of length greater than one: Due to their pairwise distance, this will never be cheaper than crossing an edge gadget along the red path, see also [21]. ◀

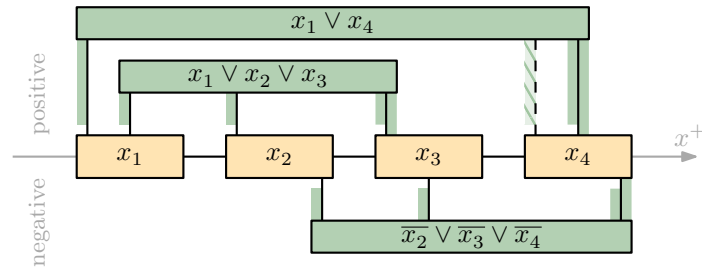
This has the following implication.

► **Corollary 3.** *Given two configurations  $C_s, C_t \in \mathcal{C}(n)$  and an integer  $k \in \mathbb{N}$ , it is NP-complete to decide whether there exists an optimal schedule  $C_s \Rightarrow C_t$  with at most  $k$  pickup (and at most  $k$  drop-off) operations.*

The reduction for (2) is significantly more involved: As  $\lambda = 0$ , the robot is effectively allowed to “teleport” across the configuration. We reduce from PLANAR MONOTONE 3SAT [13], utilizing and adapting the reduction given by Akitaya et al. [3] for the sequential sliding square problem.

► **Lemma 4.** *SINGLE ROBOT RECONFIGURATION is NP-complete for  $\lambda = 0$ .*

We reduce from PLANAR MONOTONE 3SAT, an NP-complete variant of the SAT problem, which asks whether a given Boolean formula  $\varphi$  in conjunctive normal form is satisfiable, given the following properties: First, each clause consists of at most 3 literals, all either positive or negative. Second, the clause-variable incidence graph  $G_\varphi$  admits a plane drawing in which variables are mapped to the  $x$ -axis, and all positive (resp., negative) clauses are located in the same half-plane, such that edges do not cross the  $x$ -axis, see Figure 4.

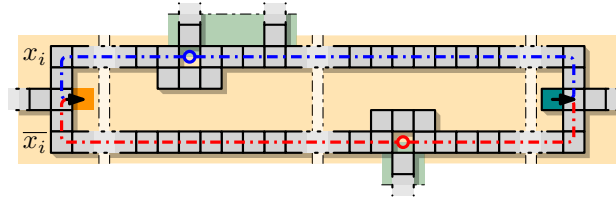


■ **Figure 4** A rectilinear embedding of the clause-variable incidence graph of the formula  $\varphi = (x_1 \vee x_3 \vee x_4) \wedge (x_1 \vee x_3) \wedge (\overline{x_2} \vee \overline{x_3} \vee \overline{x_4})$ .

We assume, without loss of generality, that each clause contains exactly three literals. Otherwise, we can extend a shorter clause with a redundant copy of one of the existing literals, e.g.,  $(x_1 \vee x_4)$  becomes  $(x_1 \vee x_4 \vee x_4)$  in Figure 4.

Our reduction maps from an instance  $\varphi$  of PLANAR MONOTONE 3SAT to an instance  $\mathcal{I}_\varphi$  of SINGLE ROBOT RECONFIGURATION such that the minimal feasible makespan  $\mathcal{I}_\varphi$  is determined by whether  $\varphi$  is satisfiable. Recall that, due to  $\lambda = 0$ , we only account for carry distance. Consider an embedding of the clause-variable incidence graph  $G_\varphi$  as above, where  $C$  and  $V$  refer to the  $m$  clauses and  $n$  variables of  $\varphi$ , respectively. We construct  $\mathcal{I}_\varphi$  as follows.

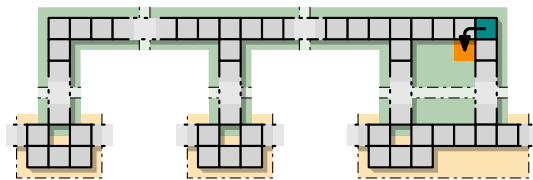
A *variable gadget* is placed on the  $x$ -axis for each  $x_i \in V$ , with gadgets connected along the axis in a straight line. Intuitively, the variable gadget asks the robot to move a specific tile west along one of two feasible paths. These paths are highlighted in red and blue in Figure 5,



■ **Figure 5** The variable gadget. The middle segments are repeated to match the incident clauses. Note the positive and negative paths (blue and red).

each of length exactly  $9(\delta(x_i) + 1)$ , where  $\delta(x_i)$  refers to the degree of  $x_i$  in the clause-variable incidence graph  $G_\varphi$ . Both paths require the robot to place its payload into the highlighted gaps to minimize the makespan, stepping over it before picking up again.

Connected to these variable gadgets are *clause gadgets*, exactly one per clause, as illustrated in Figure 6. Each clause gadget is composed of a large curve that resembles



■ **Figure 6** A clause gadget and its attachment to a variable.

an upside-down “L” attached to the  $x$ -maximal variable gadget of its literals, with three vertical *prongs* extending vertically towards variables. The prongs terminate at positions diagonally adjacent to the variable gadget of a corresponding literal. The tile at the  $90^\circ$



Proof. It is easy to observe that there is no schedule that solves a variable gadget for  $x_i$  in makespan less than  $9(\delta(x_i) + 1)$ : Building a bridge structure horizontally along the variable gadget takes a quadratic number of moves in the variable gadget's width, and shorter bridges fail to shortcut the north-south distance that the robot would otherwise cover while carrying the tile. Furthermore, we can confine tiles to their respective variable gadgets by spacing them appropriately.

Even if  $\varphi$  is not satisfiable, each variable gadget can clearly be solved in a makespan of  $9(\delta(x_i) + 1)$ . However, this no longer guarantees the existence of a cycle in every clause gadget at some point in time, leaving us to solve at least one clause gadget in a more expensive manner. In particular, we incur an extra cost of at least 4 units per unsatisfied clause, as a cycle containing the cyan tile must be created in each clause gadget before the tile can be safely picked up.

Assuming that  $m' \in (1, m]$  is the minimum number of clauses that remain unsatisfied in  $\varphi$  for any assignment of  $x_i$ , we obtain a total makespan of

$$2m + 4m' + \sum_{i=1}^n 9(\delta(x_i) + 1) = 4m' + 29m + 9n > 29m + 9n. \quad (2)$$

We conclude that a weighted makespan of  $29m + 9n$  is not achievable and must be exceeded by at least four units if the Boolean formula  $\varphi$  is not satisfiable.  $\triangleleft$

This concludes our proof of NP-completeness for  $\lambda = 0$ .  $\blacktriangleleft$

Our central complexity result Theorem 1 is simply the union of Lemmas 2 and 4.

### 3 Constant-factor approximation for 2-scaled instances

We now turn to a special case of the optimization problem in which the configurations have *disjoint bounding boxes*, i.e., there exists an axis-parallel bisector that separates the configurations. Without loss of generality, let this bisector be horizontal such that the target configuration lies south. We present an algorithm that computes schedules of makespan at most  $c \cdot \text{OPT}$  for some fixed  $c \geq 1$ .

For the remainder of this section, we additionally impose the constraint that both the start and target configurations are *2-scaled*, i.e., they consist of  $2 \times 2$ -squares of tiles aligned with a  $2 \times 2$  integer grid. In the subsequent section, we extend our result to non-scaled configurations.

► **Theorem 7.** *There exists a constant  $c$  such that for any pair of 2-scaled configurations  $C_s, C_t \in \mathcal{C}(n)$  with disjoint bounding boxes, we can efficiently compute a schedule for  $C_s \Rightarrow C_t$  with weighted makespan at most  $c \cdot \text{OPT}$ .*

Our algorithm utilizes a type of intermediate configuration called *histogram*. A histogram consists of a *base* strip of unit height and (multiple) orthogonal unit width *columns* attached to its base. The direction of its columns determines the orientation of a histogram, e.g., the histogram  $H_s$  in Figure 8 is *north-facing*.

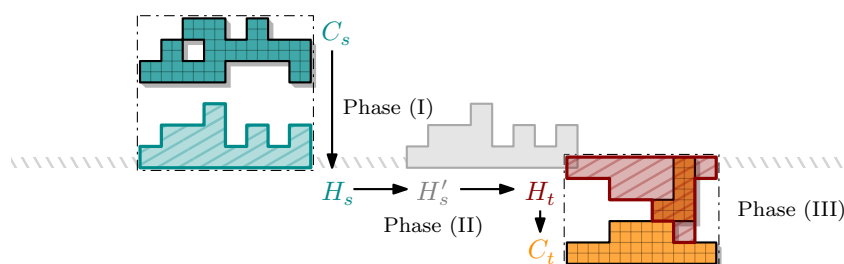
We proceed in three phases, see Figure 8 for an illustration.

**Phase (I).** Transform the configuration  $C_s$  into a north-facing histogram  $H_s$ .

**Phase (II).** Translate  $H_s$  to overlap with the target bounding box and transform it into a south-facing histogram  $H_t$  contained in the bounding box of  $C_t$ .

**Phase (III).** Finally, apply Phase (I) in reverse to obtain  $C_t$  from  $H_t$ .

We reduce this to two subroutines: Transforming any 2-scaled configuration into a 2-scaled histogram and converting any two such histograms into one another.



■ **Figure 8** An example for a start and target configuration  $C_s, C_t$ , the intermediate histograms  $H_s, H_t$  with a shared baseline, and the horizontally translated  $H'_s$  that shares a tile with  $H_t$ . If  $H_s$  and  $H_t$  overlap, we set  $H'_s := H_s$ .

### 3.1 Preliminaries for the algorithm

Before investigating the algorithm in more detail, we give some useful definitions. For two configurations  $C_s, C_t \in \mathcal{C}(n)$ , the weighted bipartite graph  $G_{C_s, C_t} = (C_s \cup C_t, C_s \times C_t, L_1)$  assigns each edge a weight corresponding to the  $L_1$ -distance between its end points.

A *perfect matching*  $M$  in  $G_{C_s, C_t}$  is a subset of edges such that every vertex is incident to exactly one of them; its weight  $w(M)$  is defined as the sum of its edge weights. By definition, there exists at least one such matching in  $G_{C_s, C_t}$ . Furthermore, a *minimum weight perfect matching* (MWPM) is a perfect matching  $M$  of minimum weight  $\sigma(C_s, C_t) = w(M)$ , which is a natural lower bound on the necessary carry distance, and thus OPT.

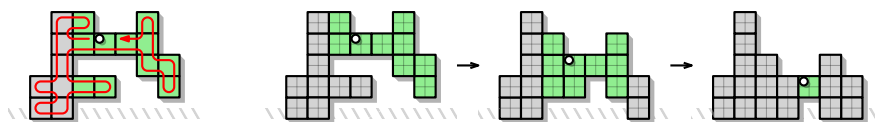
Let  $S$  be any schedule for  $C_s \Rightarrow C_t$ . Then  $S$  induces a perfect matching in  $G_{C_s, C_t}$ , as it moves every tile of  $C_s$  to a distinct position of  $C_t$ . We say that  $S$  has *optimal carry distance* exactly if  $d_C(S) = \sigma(C_s, C_t)$ .

### 3.2 Phase (I): Transform a configuration into a histogram

We proceed by constructing a histogram from an arbitrary 2-scaled configuration by moving tiles strictly in one cardinal direction.

▶ **Lemma 8.** *Let  $C_s$  be a 2-scaled polyomino and let  $H_s$  be a histogram that can be created from  $C_s$  by moving tiles in only one cardinal direction. We can efficiently compute a schedule of makespan  $\mathcal{O}(n + \sigma(C_s, H_s))$  for  $C_s \Rightarrow H_s$  with optimal carry distance.*

To achieve this, we iteratively move sets of tiles in the target direction by two units, until the histogram is constructed. We give a high-level explanation of our approach by example of a north-facing histogram, as depicted in Figure 9.



■ **Figure 9** Visualizing Lemma 8. Left: A walk across all tiles (red), the set  $H$  (gray) and free components (green). Right: Based on the walk, the free components are iteratively moved south to reach a histogram shape.

Let  $P$  be any intermediate 2-scaled polyomino obtained by moving tiles south while realizing  $C_s \Rightarrow H_s$ . Let  $H$  be the set of maximal vertical strips of tiles that contain a base tile in  $H_s$ , i.e., all tiles that do not need to be moved further south. We define the *free*

components of  $P$  as the set of connected components in  $P \setminus H$ . By definition, these exist exactly if  $P$  is not equivalent to  $H_s$ , and once a tile becomes part of  $H$ , it is not moved again until  $H_s$  is obtained.

We compute a *walk* that covers the polyomino, i.e., a path that is allowed to traverse edges multiple times and visits each vertex at least once, by depth-first traversal on an arbitrary spanning tree of  $P$ . The robot then continuously follows this walk, iteratively moving free components south and updating its path accordingly: Whenever it enters a free component  $F$  of  $P$ , we perform a subroutine (as we will describe and prove in Lemma 9) with makespan  $\mathcal{O}(|F|)$  that moves  $F$  south by two units. Adjusting the walk afterward may increase its length by  $\mathcal{O}(|F|)$  units per free component.

Upon completion of this algorithm, we can bound both the total time spent performing the subroutine and the additional cost incurred by extending the walk by  $\mathcal{O}(\sigma(C_s, H_s))$ . Taking into account the initial length of the walk, the resulting makespan is  $\mathcal{O}(n + \sigma(C_s, H_s))$ .

Before proving this result, we describe and prove the crucial subroutine for the translation of free components, that can be stated as follows.

► **Lemma 9.** *Given a free component  $F$  of a 2-scaled polyomino  $P$ , we can efficiently compute a schedule of makespan  $\mathcal{O}(|F|)$  to translate  $F$  in the target direction by two units.*

**Proof.** Without loss of generality, we assume that the target direction is south and show how to translate  $F$  south by one unit without losing connectivity. We then apply this routine twice.

We follow a bounded-length walk across  $F$  that visits exclusively tiles with a tile neighbor in northern direction. Such a walk can be computed by depth-first traversal of  $F$ . Whenever the robot enters a maximal vertical strip of  $F$  for the first time, it picks up the northernmost tile and places it at the first unoccupied position to its south.

Clearly, the sum of movements on vertical strips for carrying tiles and returning to the pre-pickup position can be bounded with  $\mathcal{O}(|F|)$ , as each strip is handled exactly once. This bound also holds for the length of the walk. ◀

By applying Lemma 9 on the whole polyomino  $P$  instead of just a free component, we can translate  $P$  in any direction with asymptotically optimal makespan.

► **Corollary 10.** *Any 2-scaled polyomino can be translated by  $k$  units in any cardinal direction by a schedule of weighted makespan  $\mathcal{O}(n \cdot k)$ .*

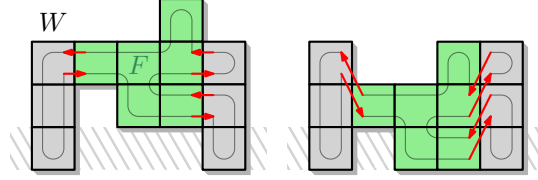
With this, we are equipped to prove the main result for the first phase.

**Proof of Lemma 8.** Without loss of generality, we assume that the target direction is south.

We start by identifying a walk  $W$  on  $C_s$  that passes every edge at most twice, by depth-first traversal of a spanning tree of  $C_s$ . To construct our schedule, we now simply move the robot along  $W$ . On this walk, we denote the  $i$ th encountered free component with  $F_i$  as follows. Whenever the robot enters a position  $t$  that belongs to a free component  $F_i$ , we move  $F_i$  south by two positions (refer to Lemma 9) and modify both  $t$  and  $W$  in accordance with the south movement that was just performed. The robot stops on the new position for  $t$  and we denote the next free component by  $F_{i+1}$ . We keep applying Lemma 9 until  $t$  does not belong to a free component, from where on the robot continues on the modified walk  $W$ . We illustrate this approach in Figure 9.

While it is clear that repeatedly moving all free components south eventually creates  $H_s$ , it remains to show that this happens within  $\mathcal{O}(n + \sigma(C_s, H_s))$  moves. To this end, we set  $F_\Sigma = \sum |F_i|$ . We first show that the schedule has a makespan in  $\mathcal{O}(n + F_\Sigma)$  and then argue that  $F_\Sigma \in \Theta(\sigma(C_s, H_s))$ . Clearly, all applications of Lemma 9 result in a makespan of  $\mathcal{O}(F_\Sigma)$ ,

and since  $|W| \in \mathcal{O}(n)$  we can also account for the number of steps on the initial walk  $W$ . However, additional steps may be required: Whenever only *parts* of  $W$  are moved south by two positions, the distance between the involved consecutive positions in  $W$  increases by two, see Figure 10. We account for these additional movements as follows.



■ **Figure 10** When all tiles in a free component  $F$  are moved south, the walk  $W$  on the polyomino may become longer.

For any free component  $F_i$ , there are at most  $2|F_i|$  edges between  $F_i$  and the rest of the configuration. Each transfer increases the movement cost by two and each edge is traversed at most twice, increasing the length of  $W$  by at most  $8|F_i|$  movements for every  $F_i$ . Consequently,  $\mathcal{O}(n + F_\Sigma)$  also accounts for these movements.

It remains to argue that  $F_\Sigma \in \Theta(\sigma(C_s, H_s))$ . Clearly, as the schedule for moving  $F_i$  two units south induces a matching with a weight in  $\Theta(|F_i|)$ , combining all these schedules induces a matching with a weight in  $\Theta(F_\Sigma)$ . We next notice that all schedules for  $C_s \Rightarrow H_s$  that move tiles exclusively south have the same weight because the sum of edge weights in the induced matchings is merely the difference between the sums over all  $y$ -positions in  $C_s$  and  $H_s$ , respectively. Finally, all these matchings have minimal weight, i.e.,  $\sigma(C_s, H_s)$ : If there exists an MWPM between  $C_s$  and  $H_s$  with crossing paths, these crossings can be removed by Observation 12 without increasing the matching's weight.

By that,  $F_\Sigma \in \Theta(\sigma(C_s, H_s))$  holds and the bound of  $\mathcal{O}(n + \sigma(C_s, H_s))$  results. Also, since Lemma 9 moves all tiles exclusively south, the schedule has optimal carry distance. ◀

### 3.3 Phase (II): Reconfigure a histogram into a histogram

It remains to show how to transform one histogram into the other. By the assumption of the existence of a horizontal bisector between the bounding boxes of  $C_s$  and  $C_t$ , the histogram  $H_s$  is north-facing, whereas  $H_t$  is south-facing. The bounding box of  $C_s$  is vertically extended to share exactly one  $y$ -coordinate with the bounding box of  $C_t$ , and this is where both histogram bases are placed; see Figure 8 for illustration. Note that the histograms may not yet overlap. However, by Corollary 10, the tiles in  $H_s$  can be moved toward  $H_t$  in asymptotically optimal makespan until both histogram bases share a tile.

► **Lemma 11.** *Let  $H_s$  be a north-facing and  $H_t$  a south-facing histogram that share at least one base tile. We can efficiently compute a schedule of makespan  $\mathcal{O}(n + \sigma(H_s, H_t))$  for  $H_s \Rightarrow H_t$  with optimal carry distance.*

To prove Lemma 11, we use a simple observation about *crossing paths*, i.e., paths that share a vertex in the integer grid. We denote by  $L_1(s, t)$  the length of a shortest path between the vertices  $s$  and  $t$ .

► **Observation 12.** *If any two shortest paths between tile positions  $s_i$  and  $t_i$  with  $i \in \{1, 2\}$  cross, then  $L_1(s_1, t_1) + L_1(s_2, t_2) \leq L_1(s_1, t_2) + L_1(s_2, t_1)$  holds.*

This follows from splitting both paths at the crossing vertex and applying triangle inequality.

**Proof of Lemma 11.** We first describe how the schedule  $S$  can be constructed and then argue that the matching induced by  $S$  is an MWPM in  $G_{H_s, H_t}$ . We conclude the proof by showing that the schedule is of size  $\mathcal{O}(n + \sigma(H_s, H_t))$ .

We write  $B_s$  and  $B_t$  for the set of all base positions in  $H_s$  and  $H_t$ , respectively, and denote the union of all base positions by  $B := B_s \cup B_t$ . We assume that all robot movements between positions in  $H_s$  and  $H_t$  are realized along a path that moves vertically until  $B$  is reached, continues horizontally on  $B$  and then moves vertically to the target position. These are shortest paths by construction.

We denote the westernmost and easternmost position in  $B$  by  $b_W$  and  $b_E$ , respectively. Without loss of generality, we assume  $b_E \in B_t$ , because this condition can always be reached by either mirroring the instance horizontally or swapping  $B_s$  and  $B_t$  and applying the resulting schedule in reverse.

First consider  $b_W \in B_s$ . We order all tiles in both  $H_s \setminus H_t$  and  $H_t \setminus H_s$  from west to east and north to south, see the left part of Figure 11. Based on this ordering,  $S$  is created by iteratively moving the first remaining tile in  $H_s \setminus H_t$  to the first remaining position in  $H_t \setminus H_s$ . This way, all moves can be realized on shortest paths over the bases.

If  $b_W \in B_t \setminus B_s$ , this is not possible as the westernmost position in  $H_t$  may not yet be reachable. Therefore, we iteratively extend  $B_s$  to the west until the western part of  $B_t$  is constructed. The tiles are taken from  $H_s$  in the same order as before, see the right part of Figure 11. Once we have moved a tile to  $b_W$ , we can continue as above with  $b_W \in B_s$ .



■ **Figure 11** Position orderings in  $H_s \setminus H_t$  and  $H_t \setminus H_s$ . Left: The main case of  $b_W \in B_s$ . Right: Additional steps are required for  $b_W \in B_t \setminus B_s$ . Tiles are moved according to the ordering, as indicated by the arrows.

Let  $M$  be the matching induced by  $S$ . We now give an iterative argument why  $M$  has the same sum of distances as an arbitrary MWPM  $M_{\text{OPT}}$  with  $w(M_{\text{OPT}}) = \sigma(H_s, H_t)$ . First consider  $b_W \in B_s$ . Given the ordering from above, we write  $s_i$  and  $t_i$  for the  $i$ th tile position in  $H_s \setminus H_t$  and  $H_t \setminus H_s$ , respectively. If  $M \neq M_{\text{OPT}}$ , there exists a minimal index  $i$  such that  $(s_i, t_i) \in M \setminus M_{\text{OPT}}$ . In  $M_{\text{OPT}}$ ,  $s_i$  and  $t_i$  are instead matched to other positions  $s_j$  and  $t_k$  with  $j, k > i$ , i.e.,  $(s_i, t_k), (s_j, t_i) \in M_{\text{OPT}}$ . Since  $j, k > i$ , the positions  $s_j$  and  $t_k$  do not lie to the west of  $s_i$  and  $t_i$ , respectively. Now note that the paths for  $(s_i, t_k)$  and  $(s_j, t_i)$  always cross: Let  $b_s$  and  $b_t$  be the positions in  $B$  that have same  $x$ -coordinates as  $s_i$  and  $t_i$ , respectively. If  $s_i$  lies to the east of  $t_i$  (case i), the path from  $s_j$  to  $t_i$  crosses  $b_s$ , and so does any path that starts in  $s_i$ . If  $s_i$  does not lie to the east of  $t_i$  (case ii), the path from  $s_i$  to  $t_k$  crosses  $b_t$ , and so does any path that ends in  $t_i$ . We illustrate both cases in Figure 12.

As the paths cross, replacing  $(s_i, t_k), (s_j, t_i)$  with  $(s_i, t_i), (s_j, t_k)$  in  $M_{\text{OPT}}$  creates a new matching  $M'_{\text{OPT}}$  with  $w(M'_{\text{OPT}}) \leq w(M_{\text{OPT}})$  due to Observation 12. By repeatedly applying this argument, we can turn  $M_{\text{OPT}}$  into  $M$  and note that  $w(M) \leq w(M_{\text{OPT}})$  holds. If  $b_W \in B_t \setminus B_s$ , case (i) applies to all tiles moved to extend  $B_s$  in western direction, and we can construct  $M$  from  $M_{\text{OPT}}$  analogously. Thus, the matching induced by  $S$  is an MWPM.

Since the carry distance  $d_C(S)$  is exactly  $\sigma(H_s, H_t)$ , it remains to bound the empty distance  $d_E(S)$  with  $\mathcal{O}(n + \sigma(H_s, H_t))$ . To this end, we combine all paths from one drop-off



■ **Figure 12** The paths for  $(s_i, t_k)$  and  $(s_j, t_i)$  cross in  $b_s$  or  $b_t$ . Left:  $s_i$  lies to the east of  $t_i$  (case i). Right:  $s_i$  does not lie to the east of  $t_i$  (case ii).

position back to its pickup position (in sum  $\sigma(H_s, H_t)$ ) with all paths between consecutive pickup locations (in sum  $\mathcal{O}(n)$  because the locations are ordered). Since the robot does not actually return to the pickup location, these paths of total length  $\mathcal{O}(n + \sigma(H_s, H_t))$  are an upper bound for  $d_E(S)$ , and we get  $|S| \in \mathcal{O}(n + \sigma(H_s, H_t))$ . ◀

### 3.4 Correctness of the algorithm

In the previous sections, we presented schedules for each phase of the overall algorithm. We will now leverage these insights to prove the main result of this section, restated here.

► **Theorem 7.** *There exists a constant  $c$  such that for any pair of 2-scaled configurations  $C_s, C_t \in \mathcal{C}(n)$  with disjoint bounding boxes, we can efficiently compute a schedule for  $C_s \Rightarrow C_t$  with weighted makespan at most  $c \cdot \text{OPT}$ .*

**Proof.** By Lemmas 8 and 11, the makespan of the three phases is bounded by  $\mathcal{O}(n + \sigma(C_s, H_s))$ ,  $\mathcal{O}(n + \sigma(H_s, H_t))$ , and  $\mathcal{O}(n + \sigma(H_t, C_t))$ , respectively, which we now bound by  $\mathcal{O}(\sigma(C_s, C_t))$ , proving asymptotic optimality for  $C_s \Rightarrow C_t$ .

Clearly,  $n \in \mathcal{O}(\sigma(C_s, C_t))$ , as each of the  $n$  tiles has to be moved due to  $C_s \cap C_t = \emptyset$ . We prove a tight bound on the remaining terms, i.e.,

$$\sigma(C_s, H_s) + \sigma(H_s, H_t) + \sigma(H_t, C_t) = \sigma(C_s, C_t). \quad (3)$$

In Phase (I), tiles are moved exclusively towards the bounding box of  $C_t$  along shortest paths to obtain  $H_s$ , so  $\sigma(C_s, C_t) = \sigma(C_s, H_s) + \sigma(H_s, C_t)$ . The same applies to the reverse of Phase (III), i.e.,  $\sigma(C_t, H_s) = \sigma(C_t, H_t) + \sigma(H_t, H_s)$ . Due to symmetry of the lower bound, Equation (3) immediately follows. The total makespan is thus in  $\mathcal{O}(\sigma(C_s, C_t)) = \mathcal{O}(\text{OPT})$ . ◀

Lemmas 8 and 11 establish schedules that minimize the carry distance and Equation (3) ensures that the combined paths remain shortest possible. Thus, the provided schedule has optimal carry distance. In particular, we obtain an optimal schedule when  $\lambda = 0$ , which corresponds to the case where the robot incurs no cost for movement when not carrying a tile.

► **Corollary 13.** *For any pair of 2-scaled configurations  $C_s, C_t \in \mathcal{C}(n)$  with disjoint bounding boxes and  $\lambda = 0$ , we can efficiently compute an optimal schedule for  $C_s \Rightarrow C_t$ .*

## 4 Constant-factor approximation for general instances

The key advantage of 2-scaled instances is the absence of cut vertices, which simplifies the maintenance of connectivity during the reconfiguration. Therefore, the main challenge in reconfiguring general instances lies in managing cut vertices.

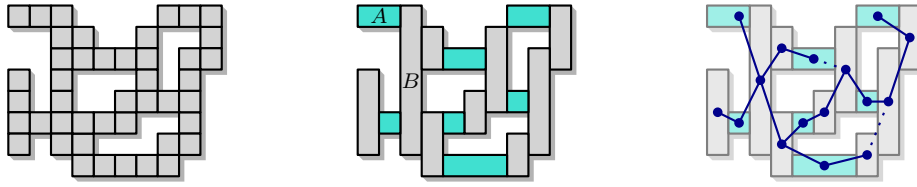
Most parts of our previous method already work independent of the configuration scale. Thus, the only modification required concerns Lemma 9, as the polyomino may become

disconnected while moving free components that are not 2-scaled. To address this, Lemma 14 introduces an alternative strategy for translating free components by a single unit while maintaining connectivity throughout the process. The key observation is that two auxiliary tiles can be used to preserve local connectivity around the cut vertices that need to be moved. The use of auxiliary tiles to preserve connectivity is also exploited in other models [2, 34].

To simplify the arguments, we assume that the robot is capable of holding up to two auxiliary tiles, but will later explain how to modify the strategy to work with no more than a single auxiliary tile.

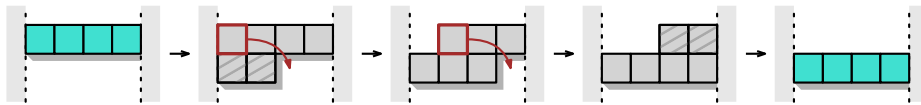
► **Lemma 14.** *Let the robot hold two auxiliary tiles. Given a free component  $F$  on a polyomino  $P$ , we can efficiently compute a schedule of makespan  $\mathcal{O}(|F|)$  to translate  $F$  in the target direction by one unit.*

Before proving this, we give a high-level description of the approach. Without loss of generality, we translate  $F$  in southern direction. We decompose  $F$  into maximal vertical *strips* of unit width and maximal horizontal *corridors* of unit height, that we collectively refer to as the *elements* of  $F$ , as visualized in Figure 13. In particular, strips that only consist of a single tile are grouped with adjacent single tiles (if they exist) and become maximal horizontal corridors. We will show that we are able to translate both types of elements one



■ **Figure 13** A decomposition of a polyomino (left) into gray strips and cyan corridors (center). From that, we create an adjacency graph  $G$  and (by leaving out dotted edges) a spanning tree  $T$  (right).

unit to the south, possibly with the support of auxiliary tiles, while retaining connectivity within the respective elements. Because of the cut vertices, the most challenging part are corridors that consist of at least two tiles. Figure 14 illustrates how two auxiliary tiles can be used to translate a corridor one unit south.



■ **Figure 14** The steps of moving a corridor of width 4 south, using two auxiliary tiles.

Strips can be translated south without the use of auxiliary tiles. Because translating a single element may cause disconnection to adjacent elements, we apply a recursive strategy that first handles the elements *blocking* our translation. We then move our current element, and finally process all other adjacent elements.

**Proof of Lemma 14.** We refer to the aforementioned decomposition of a polyomino into strips and corridors. In this construction, each corridor is adjacent to up to two strips and each strip has a height of at least 2. Furthermore, all adjacency is either to the west or east side, but never vertical. Note that because  $F$  is connected, the graph  $G = (V, E)$  of adjacent elements is connected as well.

We now compute an arbitrary spanning tree  $T$  from  $G$ ; and for the remainder of the proof, adjacency of elements is considered to be in  $T$ . For two adjacent elements  $A, B \in V$ , we say that  $A$  *blocks*  $B$ , if translating all tiles in  $B$  south by one unit would result in all tiles of  $A$  losing adjacency to  $B$ . An example for an element  $A$  blocking and element  $B$  is illustrated in Figure 13: if we translate  $B$  south, we disconnect  $A$  from the polyomino. Note that  $A$  blocks  $B$  exactly if the northernmost tile in  $B$  has the same height as the southernmost tile in  $A$ . As at least one of  $A$  or  $B$  is a strip (with height at least 2),  $A$  and  $B$  cannot block one another simultaneously. Because we translate every tile south by only a single unit, we do not need to update  $T$ , which means that if  $A$  blocks  $B$ , then once  $A$  has been moved south one step,  $B$  can be moved south as well without  $A$  and  $B$  losing connectivity. If  $A$  and  $B$  are not blocking one another, they can be moved south in any order.

We next look at how to move an element  $A$  south in the case that  $A$  is not blocked by any adjacent element. We use two auxiliary tiles which the robot holds at the beginning and end of the operation. If  $A$  is a strip or a single-tile corridor, we place one tile south of  $A$  and then remove the northernmost tile. If  $A$  is a corridor of two or more tiles, we place the two auxiliary tiles right below the two westernmost tiles of  $A$ . We then move each tile by two steps to the east and one position south, starting from the east. The last two tiles become new auxiliary tiles; see Figure 14. Clearly, moving  $A$  south has makespan  $\mathcal{O}(|A|)$ .

Finally, the robot has to traverse  $T$  such that every element is moved south only after its adjacent blocking elements. This can be done recursively, starting at any element in  $T$  in the following way. At the current element  $A$ :

1. Recurse on all adjacent elements that block  $A$  and are not moved south yet.
2. Move  $A$  south.
3. Recurse on the remaining unvisited elements adjacent to  $A$ .

Because  $T$  is connected, every element is visited with this strategy. By ordering the adjacent elements, each recursion on an element  $A$  requires only  $\mathcal{O}(|A|)$  additional movements to move towards the corresponding elements.

It remains to show that no element is recursed on more than once. Assume that some element  $B$  is recursed on twice. As there are no cycles in  $T$  and all unvisited or blocking neighbors are recursed on in each invocation,  $B$  can only be recursed on for a second time by some element  $A$  which was previously recursed on by  $B$ . This second invocation stems from the first step of handling  $A$  because the third step excludes visited elements, which means that  $B$  blocks  $A$ , and  $B$  is not moved south. Thus, the first invocation on  $B$  did not yet reach the second step. In other words, the recursive call on  $A$  resulted from  $A$  blocking  $B$ . This is a contradiction, as  $A$  and  $B$  cannot mutually block one another. ◀

It remains to argue how two auxiliary tiles can be obtained and emulated in our model. By doing so, we obtain the following.

► **Theorem 15.** *There exists a constant  $c$  such that for any pair of configurations  $C_s, C_t \in \mathcal{C}(n)$  with disjoint bounding boxes, we can efficiently compute a schedule for  $C_s \Rightarrow C_t$  with weighted makespan at most  $c \cdot OPT$ .*

**Proof.** The idea is to execute Lemma 14 instead of Lemma 9 every time it is required in Theorem 7. To this end, we explain the required modifications for Lemma 8; the same adaptations also work for  $H_s \Rightarrow H'_s$ . Before we translate the first free component  $F$ , we move two additional tiles to  $F$ . These tiles can be any tiles from  $C_s$  that are not necessary for connectivity (e.g., any leaf from a spanning tree of the dual graph of  $C_s$ ). Obtaining these auxiliary tiles requires  $\mathcal{O}(n)$  movements. Next, we need to sequentially move both tiles from

one free component to the next whenever we continue our walk on the configuration. We can bound these steps with the length of the walk, thus requiring  $\mathcal{O}(n)$  movements in sum.

Now, we only have to argue that Lemma 14 still holds if the robot initially carries a single tile and must not carry more than one tile at a time: Whenever the robot finishes translating the current element, it only picks up one of the two auxiliary tiles and moves it to the next unvisited element. This tile is placed in an adjacent position to the target direction of this element (which must be free). The robot then moves back and picks up the other auxiliary tile. As this extra movement requires  $\mathcal{O}(|F|)$  additional moves in total, the makespan of Lemma 14 is still in  $\mathcal{O}(|F|)$ .

With these adaptations, we can apply Lemma 14 instead of Lemma 9 in Theorem 7. Moreover, the makespan of Lemma 8 still lies in  $\mathcal{O}(n + \sigma(C_s, H_s))$ . By that, the analysis of the overall makespan is identical to Theorem 7. The only difference is that schedules created by Lemma 14 do not necessarily have optimal carry distance, which also applies to the overall schedule. ◀

## 5 Discussion

In this paper, we presented progress on the reconfiguration problem for tile-based structures (i.e., polyominoes) within abstract material-robot systems. In particular, we showed that the problem is NP-complete for any weighting between moving with or without carrying a tile.

Complementary to this negative result, we developed an algorithm to reconfigure two polyominoes into one another in the case that both configurations are contained in disjoint bounding boxes. The computed schedules are within a constant factor of the optimal reconfiguration schedule. It is easy to see that our approach can also be used to construct a polyomino, rather than reconfigure one into another. Instead of deconstructing a start configuration to generate building material, we can assume that tiles are located within a “depot” from which they can be picked up. Performing the second half of the algorithm works as before and builds the target configuration out of tiles from the depot.

Several open questions remain. A natural open problem is to adapt the approach to instances in which the bounding boxes of the configurations intersect, i.e., they overlap, or are nested. Furthermore, it seems plausible that our methods can be generalized to be performed by many robots in parallel. Much more intricate is the question on whether a fully distributed approach is possible.

---

## References

- 1 Zachary Abel, Hugo A. Akitaya, Scott Duke Kominers, Matias Korman, and Frederick Stock. A universal in-place reconfiguration algorithm for sliding cube-shaped robots in a quadratic number of moves. In *Symposium on Computational Geometry (SoCG)*, pages 1:1–1:14, 2024. doi:10.4230/LIPICS.SOCG.2024.1.
- 2 Hugo A. Akitaya, Esther M. Arkin, Mirela Damian, Erik D. Demaine, Vida Dujmovic, Robin Y. Flatland, Matias Korman, Belén Palop, Irene Parada, André van Renssen, and Vera Sacristán. Universal reconfiguration of facet-connected modular robots by pivots: The  $O(1)$  musketeers. *Algorithmica*, 83:1316–1351, 2021. doi:10.1007/s00453-020-00784-6.
- 3 Hugo A. Akitaya, Erik D. Demaine, Matias Korman, Irina Kostitsyna, Irene Parada, Willem Sonke, Bettina Speckmann, Ryuhei Uehara, and Jules Wulms. Compacting squares: Input-sensitive in-place reconfiguration of sliding squares. In *Scandinavian Symposium on Algorithm Theory (SWAT)*, pages 4:1–4:19, 2022. doi:10.4230/LIPICS.SWAT.2022.4.

- 4 Hugo A. Akitaya, Sándor P. Fekete, Peter Kramer, Saba Molaei, Christian Rieck, Frederick Stock, and Tobias Wallner. Sliding squares in parallel, 2024. Submitted for publication. doi:10.48550/arXiv.2412.05523.
- 5 Abdullah Almethen, Othon Michail, and Igor Potapov. Pushing lines helps: Efficient universal centralised transformations for programmable matter. *Theoretical Computer Science*, 830:43–59, 2020. doi:10.1016/j.tcs.2020.04.026.
- 6 Abdullah Almethen, Othon Michail, and Igor Potapov. On efficient connectivity-preserving transformations in a grid. *Theoretical Computer Science*, 898:132–148, 2022. doi:10.1016/j.tcs.2022.09.016.
- 7 Aaron T. Becker, Sándor P. Fekete, Phillip Keldenich, Dominik Krupke, Christian Rieck, Christian Scheffer, and Arne Schmidt. Tilt assembly: Algorithms for micro-factories that build objects with uniform external forces. *Algorithmica*, 82(2):165–187, 2020. doi:10.1007/S00453-018-0483-9.
- 8 Aaron T. Becker, Sándor P. Fekete, Li Huang, Phillip Keldenich, Linda Kleist, Dominik Krupke, Christian Rieck, and Arne Schmidt. Targeted drug delivery: Algorithmic methods for collecting a swarm of particles with uniform, external forces. In *International Conference on Robotics and Automation (ICRA)*, pages 2508–2514, 2020. doi:10.1109/ICRA40945.2020.9196551.
- 9 Mohamed Khalil Ben-Larbi, Kattia Flores Pozo, Tom Haylok, Mirue Choi, Benjamin Grzesik, Andreas Haas, Dominik Krupke, Harald Konstanski, Volker Schaus, Sándor P. Fekete, Christian Schurig, and Enrico Stoll. Towards the automated operations of large distributed satellite systems. Part 1: Review and paradigm shifts. *Advances in Space Research*, 67(11):3598–3619, 2021. doi:10.1016/j.asr.2020.08.009.
- 10 Christopher G. Cameron, Zach Fredin, and Neil Gershenfeld. Discrete assembly of unmanned aerial systems. In *International Conference on Unmanned Aircraft Systems (ICUAS)*, pages 339–344, 2022. doi:10.1109/ICUAS54217.2022.9836082.
- 11 Kenneth C. Cheung and Neil Gershenfeld. Reversibly assembled cellular composite materials. *Science*, 341(6151):1219–1221, 2013. doi:10.1126/science.1240889.
- 12 Matthew Connor and Othon Michail. Transformation of modular robots by rotation: 3 + 1 musketeers for all orthogonally convex shapes. *Journal of Computer and System Sciences*, 150:103618, 2025. doi:10.1016/j.jcss.2024.103618.
- 13 Mark de Berg and Amirali Khosravi. Optimal binary space partitions for segments in the plane. *International Journal on Computational Geometry and Applications*, 22(3):187–206, 2012. doi:10.1142/S0218195912500045.
- 14 Sándor P. Fekete. Coordinating swarms of objects at extreme dimensions. In *International Workshop on Combinatorial Algorithms (IWOCA)*, pages 3–13, 2020. doi:10.1007/978-3-030-48966-3\_1.
- 15 Sándor P. Fekete, Phillip Keldenich, Ramin Kosfeld, Christian Rieck, and Christian Scheffer. Connected coordinated motion planning with bounded stretch. *Autonomous Agents and Multi-Agent Systems*, 37(2), 2023. doi:10.1007/S10458-023-09626-5.
- 16 Sándor P. Fekete, Peter Kramer, Christian Rieck, Christian Scheffer, and Arne Schmidt. Efficiently reconfiguring a connected swarm of labeled robots. *Autonomous Agents and Multi-Agent Systems*, 38(2), 2024. doi:10.1007/s10458-024-09668-3.
- 17 Sándor P. Fekete, Eike Niehs, Christian Scheffer, and Arne Schmidt. Connected reconfiguration of lattice-based cellular structures by finite-memory robots. *Algorithmica*, 84(10):2954–2986, 2022. doi:10.1007/s00453-022-00995-z.
- 18 Robert Fitch, Zack J. Butler, and Daniela Rus. Reconfiguration planning for heterogeneous self-reconfiguring robots. In *International Conference on Intelligent Robots and Systems (IROS)*, pages 2460–2467, 2003. doi:10.1109/IROS.2003.1249239.
- 19 Robert Fitch, Zack J. Butler, and Daniela Rus. Reconfiguration planning among obstacles for heterogeneous self-reconfiguring robots. In *International Conference on Robotics and Automation (ICRA)*, pages 117–124, 2005. doi:10.1109/ROBOT.2005.1570106.

- 20 Javier Garcia, Michael Yannuzzi, Peter Kramer, Christian Rieck, and Aaron T. Becker. Connected reconfiguration of polyominoes amid obstacles using RRT\*. In *International Conference on Intelligent Robots and Systems (IROS)*, pages 6554–6560, 2022. doi:10.1109/IROS47612.2022.9981184.
- 21 Javier Garcia, Michael Yannuzzi, Peter Kramer, Christian Rieck, Sándor P. Fekete, and Aaron T. Becker. Reconfiguration of a 2D structure using spatio-temporal planning and load transferring. In *International Conference on Robotics and Automation (ICRA)*, pages 8735–8741, 2024. doi:10.1109/ICRA57147.2024.10611057.
- 22 Robert Gmyr, Kristian Hinnenthal, Irina Kostitsyna, Fabian Kuhn, Dorian Rudolph, and Christian Scheideler. Shape recognition by a finite automaton robot. In *International Symposium on Mathematical Foundations of Computer Science (MFCS)*, pages 52:1–52:15, 2018. doi:10.4230/LIPIcs.MFCS.2018.52.
- 23 Robert Gmyr, Kristian Hinnenthal, Irina Kostitsyna, Fabian Kuhn, Dorian Rudolph, Christian Scheideler, and Thim Strothmann. Forming tile shapes with simple robots. *Natural Computing*, 19(2):375–390, 2020. doi:10.1007/s11047-019-09774-2.
- 24 Christine E. Gregg, Damiana Catanoso, Olivia Irene B. Formoso, Irina Kostitsyna, Megan E. Ochalek, Taiwo J. Olatunde, In Won Park, Frank M. Sebastianelli, Elizabeth M. Taylor, Greenfield T. Trinh, and Kenneth C. Cheung. Ultralight, strong, and self-reprogrammable mechanical metamaterials. *Science Robotics*, 9(86), 2024. doi:10.1126/scirobotics.adi2746.
- 25 Christine E. Gregg, Joseph H. Kim, and Kenneth C. Cheung. Ultra-light and scalable composite lattice materials. *Advanced Engineering Materials*, 20(9):1800213, 2018. doi:10.1002/adem.201800213.
- 26 Kristian Hinnenthal, David Liedtke, and Christian Scheideler. Efficient shape formation by 3D hybrid programmable matter: An algorithm for low diameter intermediate structures. In *Symposium on Algorithmic Foundations of Dynamic Networks (SAND)*, pages 15:1–15:20, 2024. doi:10.4230/LIPICS.SAND.2024.15.
- 27 Alon Itai, Christos H. Papadimitriou, and Jayme Luiz Szwarcfiter. Hamilton paths in grid graphs. *SIAM Journal on Computing*, 11(4):676–686, 1982. doi:10.1137/0211056.
- 28 Ben Jenett and Kenneth Cheung. BILL-E: Robotic platform for locomotion and manipulation of lightweight space structures. In *Adaptive Structures Conference (ASC)*, 2017. doi:10.2514/6.2017-1876.
- 29 Benjamin Jenett, Amira Abdel-Rahman, Kenneth Cheung, and Neil Gershenfeld. Material-robot system for assembly of discrete cellular structures. *IEEE Robotics and Automation Letters*, 4(4):4019–4026, 2019. doi:10.1109/LRA.2019.2930486.
- 30 Benjamin Jenett, Daniel Cellucci, Christine Gregg, and Kenneth Cheung. Meso-scale digital materials: modular, reconfigurable, lattice-based structures. In *International Manufacturing Science and Engineering Conference (MSEC)*, 2016. doi:10.1115/MSEC2016-8767.
- 31 Benjamin Jenett, Christine Gregg, Daniel Cellucci, and Kenneth Cheung. Design of multifunctional hierarchical space structures. In *Aerospace Conference*, pages 1–10, 2017. doi:10.1109/AERO.2017.7943913.
- 32 Matthias Konitzny, Yitong Lu, Julien Leclerc, Sándor P. Fekete, and Aaron T. Becker. Gathering physical particles with a global magnetic field using reinforcement learning. In *International Conference on Intelligent Robots and Systems (IROS)*, pages 10126–10132, 2022. doi:10.1109/IROS47612.2022.9982256.
- 33 Irina Kostitsyna, Tim Ophelders, Irene Parada, Tom Peters, Willem Sonke, and Bettina Speckmann. Optimal in-place compaction of sliding cubes. In *Scandinavian Symposium on Algorithm Theory (SWAT)*, pages 31:1–31:14, 2024. doi:10.4230/LIPICS.SWAT.2024.31.
- 34 Othon Michail, George Skretas, and Paul G. Spirakis. On the transformation capability of feasible mechanisms for programmable matter. *Journal of Computer and System Sciences*, 102:18–39, 2019. doi:10.1016/j.jcss.2018.12.001.
- 35 Eike Niehs, Arne Schmidt, Christian Scheffer, Daniel E. Biediger, Michael Yannuzzi, Benjamin Jenett, Amira Abdel-Rahman, Kenneth C. Cheung, Aaron T. Becker, and Sándor P. Fekete.

- Recognition and reconfiguration of lattice-based cellular structures by simple robots. In *International Conference on Robotics and Automation (ICRA)*, pages 8252–8259, 2020. doi: 10.1109/ICRA40945.2020.9196700.
- 36 Ana L. Santos, Dongdong Liu, Anna K. Reed, Aaron M. Wyderka, Alexis van Venrooy, John T. Li, Victor D. Li, Mikita Misiura, Olga Samoylova, Jacob L. Beckham, Ciceron Ayala-Orozco, Anatoly B. Kolomeisky, Lawrence B. Alemany, Antonio Oliver, George P. Tegos, and James M. Tour. Light-activated molecular machines are fast-acting broad-spectrum antibacterials that target the membrane. *Science Advances*, 8(22):eabm2055, 2022. doi: 10.1126/sciadv.abm2055.
- 37 Zhuoran Zhang, Xian Wang, Jun Liu, Changsheng Dai, and Yu Sun. Robotic micromanipulation: Fundamentals and applications. *Annual Review of Control, Robotics, and Autonomous Systems*, 2:181–203, 2019. doi:10.1146/ANNUREV-CONTROL-053018-023755.
- 38 Yangsheng Zhu, Mingjing Qi, Zhiwei Liu, Jianmei Huang, Dawei Huang, Xiaojun Yan, and Liwei Lin. A 5-mm untethered crawling robot via self-excited electrostatic vibration. *IEEE Transactions on Robotics*, 38(2):719–730, 2022. doi:10.1109/TR0.2021.3088053.